The Impact of Normal Magnetic Fields on Instability of Thermocapillary Convection in a Two-Layer Fluid System

Hulin Huang[1]
e-mail: hlhuang@nuaa.edu.cn

Xiaoming Zhou

Academy of Frontier Science,
Nanjing University of Aeronautics and Astronautics,
Nanjing, 210016, P.R. China

When a temperature gradient is imposed along a liquid-liquid interface, thermocapillary convection is driven by the surface tension gradient. Such flow occurs in many application processes, such as thin-film coating, metal casting, and crystal growth. In this paper, the effect of a normal magnetic field, which is perpendicular to the interface, on the instability of thermocapillary convection in a rectangular cavity with differentially heated sidewalls, filled with two viscous, immiscible, incompressible fluids, is studied under the absence of gravity. In the two-layer fluid system, the upper layer fluid is electrically nonconducting encapsulant B_2O_3, while the underlayer fluid is electrically conducting molten InP. The interface between the two fluids is assumed to be flat and nondeformable. The results show that the two-layer fluid system still experiences a wavelike state when the magnetic field strength B_z is less than 0.04 T. The wave period increases and the amplitude decreases with the increasing of magnetic field strength. However, the convective flow pattern becomes complicated with a variable period, while the perturbation begins to fall into oblivion as the magnetic field intensity is larger than 0.05 T. When $B_z=0.1$ T, the wavelike state does not occur, the thermocapillary convection instability is fully suppressed, and the unsteady convection is changed to a steady thermocapillary flow. [DOI: 10.1115/1.3084211]

Keywords: horizontal temperature gradient, thermocapillary convection, magnetohydrodynamics, wavelike state, magnetic fields, two-layer fluid system

1 Introduction

The study of two-layer fluid thermocapillary convection is of great importance in many engineering applications, including thin-film coating, metal casting, and crystal growth. In these types of flow, a nonuniform temperature distribution at the fluid interface induces interfacial tension gradients that, in turn, generate a driving force for thermocapillary convection (also known as Marangoni convection). The phenomena can cause adverse effects in several manufacturing processes, i.e., imperfections in crystal growth, and thus have attracted much interest. Smith and Davis [1] (S&D hereafter) performed a linear stability analysis on a thermocapillary flow in an infinite liquid layer with a constant-temperature gradient along a free surface. They predicted that the hydrothermal wave instability was a kind of new instability. Afterwards, the hydrothermal wave was confirmed by many reports. Riley and Neitzel [2] experimentally proved the existence of the hydrothermal wave, the characteristics of which were similar to the analysis by S&D. Xu and Zebib [3] made a numerical simulation on thermocapillary convection in a cavity including the influence of sidewalls, and they obtained a standing wave consisting of a pair of hydrothermal waves. Burguete et al. [4] reported experiments on buoyant-thermocapillary instabilities in differentially heated liquid layers. Depending on the height of liquid and on the aspect ratio, the two-dimensional basic flow destabilized into oblique traveling waves or longitudinal stationary rolls, respectively, for small and large fluid heights. The magnetic field has been motivated as one of the ways to further control free surface fluid flows. In particular, a magnetic field was applied to damp the flow in growing single crystals. Yang and Ma [5] investigated the impact of a magnetic field on the natural convection in a two-layer fluid system. Their results showed that the magnetic field provided an electromagnetic damping of the molten semiconductor in the lower layer fluid. Morthland and Walker [6] studied the effect of a magnetic field on the thermocapillary convection of the floating zone in a microgravity environment. The authors thought that a strong magnetic field parallel to the free surface of the floating zone could eliminate the unsteady convection associated with the hydrothermal rolls. Rao and Biswal [7] investigated the effect of a uniform magnetic field on the Benard–Marangoni convection in a shallow cavity. The results indicated that it was possible to control the convection in the lower layer by a suitable choice of the magnetic field.

Thermocapillary convection in a single fluid layer confined within a differentially heated rectangular cavity has been one of the most widely studied problems associated with the crystal growth process. Since encapsulation may be used to reduce the strength of steady thermocapillary convection, Liu et al. [8] extended their studies to the case of immiscible double liquid layers with the imposed temperature gradient parallel to the free surface. However, in comparison with the unencapsulated process, modeling of liquid-encapsulated crystal growth has received considerably less attention and the effect of magnetic fields on the stability of this flow remains an open question. Based on the fact that an applied external magnetic field does effectively suppress the thermocapillary convection instability, so, in this paper, we conducted a three-dimensional numerical simulation to investigate the effect of external magnetic fields on the instability of thermocapillary flow in a two-layer fluid system in a rectangular cavity under the absence of gravity.

[1]Corresponding author.

Contributed by the Heat Transfer Division of ASME for publication in the JOURNAL OF HEAT TRANSFER. Manuscript received January 29, 2008; final manuscript received November 9, 2008; published online April 7, 2009. Review conducted by Cholik Chan.

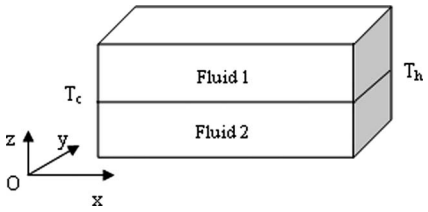

Fig. 1 Physical model

Table 1 Thermophysical properties of molten InP and B_2O_3

Property	Molten InP	B_2O_3
Viscosity (Pa s)	8.19×10^{-4}	3.9
Density (kg/m^3)	5050.0	1648.0
Specific heat (J/kg K)	424.0	1830.0
Thermal conductivity (W/m K)	22.0	2.0
Electrical conductivity (Ω^{-1} m^{-1})	7.0×10^5	0.0
Interfacial tension temperature coefficient (N/m K)	-1.2×10^{-3}	

2 Physical and Mathematical Models

The three-dimensional convective motion domain is a rectangular cavity as shown in Fig. 1 with a length (x) of 40 mm, a depth (y) of 20 mm, and a height (z) of 20 mm, respectively. The cavity is filled with two horizontal layers of immiscible fluids and each liquid layer height is 10 mm. The upper layer fluid is encapsulant boron oxide (B_2O_3) and the underlayer fluid is molten indium-phosphide (InP). The right wall is maintained at a constant-temperature T_h, while the left wall is at a lower temperature T_c ($T_h > T_c$). All the other walls are considered to be adiabatic. The temperature gradient is along the interface from right to left, the characteristic length is $L=40$ mm based on the interfacial length, which is significant for the wave traveling, and the aspect ratio Γ for each fluid is 4. The assumptions made in our model are as follows: (1) The two kinds of fluids are incompressible Newtonian fluids, (2) the flow is laminar flow, (3) the interface is flat and nondeformable, and (4) all the walls are electrically nonconducting. With the above assumptions, the momentum and energy equations are expressed as follows (subscript $i=1$ or 2, and 1 denotes the upper layer and 2 denotes the lower layer):

$$\nabla \cdot \boldsymbol{v}_i = 0 \tag{1}$$

$$\frac{\partial \boldsymbol{v}_i}{\partial t} + \boldsymbol{v}_i \cdot \nabla \boldsymbol{v}_i = -\frac{1}{\rho_i}\nabla p_i + \nu_i \nabla^2 \boldsymbol{v}_i + \frac{1}{\rho_i}\boldsymbol{f}_i \tag{2}$$

$$\frac{\partial T_i}{\partial t} + \boldsymbol{v}_i \cdot \nabla T_i = \alpha_i \nabla^2 T_i \tag{3}$$

where Lorentz force is expressed as $\boldsymbol{f}_i = \boldsymbol{J}\times\boldsymbol{B}$. $\boldsymbol{B}$ is the magnetic field intensity, which includes both the applied ($\boldsymbol{B}_z$) and induced magnetic field ($\boldsymbol{b}$) components. $\boldsymbol{J}$ is induced current density.

The induced magnetic field $\boldsymbol{b}$ can be derived from Maxwell's equations and Ohm's law as follows:

$$\frac{\partial \boldsymbol{b}}{\partial t} + (\boldsymbol{v}\cdot\nabla)\boldsymbol{b} = \frac{1}{\mu_m \sigma_m}\nabla^2 \boldsymbol{b} + (\boldsymbol{B}\cdot\nabla)\boldsymbol{v} \tag{4}$$

The induced current density is $\boldsymbol{J} = 1/\mu_m(\nabla\times\boldsymbol{B})$.

2.1 Boundary Conditions . All the walls are the no slip conditions and

$$T = T_c, \quad \boldsymbol{J}_x = 0 \quad \text{at} \quad x = 0 \tag{5a}$$

$$T = T_h, \quad \boldsymbol{J}_x = 0 \quad \text{at} \quad x = L \tag{5b}$$

$$\frac{\partial T}{\partial t} = 0, \quad \boldsymbol{J}_z = 0 \quad \text{at} \quad z = 0 \quad \text{and} \quad L/2 \tag{5c}$$

$$\frac{\partial T}{\partial t} = 0, \quad \boldsymbol{J}_y = 0 \quad \text{at} \quad y = 0 \quad \text{and} \quad L/2 \tag{5d}$$

The boundary conditions at the interface (at $z=L/4$)

$$u_1 = u_2, \quad v_1 = v_2, \quad w_1 = w_2 = 0 \tag{6a}$$

$$\mu_1\frac{\partial u_1}{\partial z} - \mu_2\frac{\partial u_2}{\partial z} = \frac{\partial \sigma_T}{\partial T}\frac{\partial T_2}{\partial x}, \quad \mu_1\frac{\partial v_1}{\partial z} - \mu_2\frac{\partial v_2}{\partial z} = \frac{\partial \sigma_T}{\partial T}\frac{\partial T_2}{\partial y} \tag{6b}$$

$$T_1 = T_2, \quad k_1\frac{\partial T_1}{\partial z} = k_2\frac{\partial T_2}{\partial z} \tag{6c}$$

$$\boldsymbol{J}_n = 0 \tag{6d}$$

To make sure that the oscillatory thermocapillary flow occurs in the two-layer fluid system in this paper, a $\Delta T = T_h - T_c = 15$ K corresponding to $\mathrm{Ma} = 8.79\times10^4$ was chosen; Ma represents the ratio of thermocapillary convection to conduction heat transfer. The physical properties of the fluids are the same as in Table 1.

3 Computational Method

The fundamental equations are discretized by the finite volume method. The central difference approximation is applied to the diffusion terms, while the second order upwind scheme is used for the convective terms. The discretized equations are solved by a fully implicit method in time marching. The pressure-implicit with splitting of operators (PISO) algorithm is used to handle the pressure-velocity coupling. The calculations are carried out on a nonuniform staggered grid system. Validation of the code for the oscillatory thermocapillary flow simulation was carefully done by comparing our simulation solutions with the experimental results by Schwabe and Benz [9]. Figure 2 shows the comparing of temperature oscillation frequency at a monitoring point. It indicates that the trend of simulation results is similar with the experimental results well.

The test cavity is discretized with a nonuniform mesh of $81^x \times 41^y \times 41^z$. A finer mesh gradation is utilized in regions where strong velocity and temperature gradients are anticipated. This includes regions near the solid boundaries, as well as the interface. This mesh is determined by refining the mesh size until convergence and constancy of temperature oscillatory frequency are achieved. In order to check the grid convergence, simulations with three sets of different meshes, as shown in Table 2, are performed at $\Delta T = 15$ K. Three sets of grids produced similar flow patterns

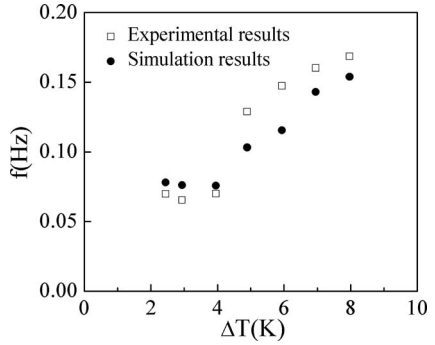

Fig. 2 Comparison of temperature oscillation frequency at a monitoring point

Table 2 Mesh dependency of temperature oscillation frequency at monitoring point *P*

Mesh	$81^x \times 41^y \times 41^z$	$91^x \times 46^y \times 46^z$	$101^x \times 51^y \times 51^z$
Frequency (Hz)	0.232511	0.232558	0.232603

and oscillation characteristics. However, the frequency of temperature oscillation at the monitoring point P of interface ($x=20$ mm, $y=10$ mm, and $z=10$ mm) showed small grid dependence. In addition, when magnetic field is applied, the calculations are repeated with a $101^x \times 51^y \times 51^z$ grid. The numerical solutions show for both grids the same qualitative behavior and differ quantitatively by less than 5%. Therefore, the mesh elected in this study is sufficient for accurate simulation. Based on Leboucher's [10] study, to achieve a stable numerical solution throughout the simulation the time step should be reduced when a magnetic field is applied. So the adaptive time step is used and varies between 1×10^{-4} and 1×10^{-2}. For each time step the quotient $Q=|\varphi^{n+1}-\varphi^n|/|\varphi^n_{\max}|$ is calculated for all dependent variables in all grid points. The index $n+1$ denotes a discrete point of time, which follows the point of time n after a time step Δt. If $Q\leq10^{-5}$ is valid for all variables in all grid points the solution is interpreted as converged.

4 Results and Discussions

Numerical simulations for the effect of normal magnetic field on the instability of thermocapillary convection were performed in the present work. The upper layer fluid is encapsulant and the underlayer fluid is molten semiconductor. Here, the convection in the underlayer fluid is our concern because of its role in practical engineering.

4.1 Thermocapillary Convection Instability Without Magnetic Field. Any temperature difference ($\Delta T>0$) produces a surface tension gradient at the interface between the molten liquid and the encapsulant and the Marangoni effect induces thermocapillary flows in two fluids. The thermocapillary flow of each fluid layer (aspect ratio $\Gamma=4$) appears as a steady flow with a single convective cell when ΔT is very small, which is called as the "basic flow." However, when ΔT exceeds a certain threshold value, this basic flow will change to oscillatory convection.

Figure 3 exhibits the streamlines' pattern of the oscillatory thermocapillary convection in one period at $\mathrm{Ma}=8.79\times10^4$. When $t=\tau_0$, it is an initial pattern of a periodical oscillatory flow in the two-layer fluids, where τ_0 is the starting time of temperature oscillation. The cell near the cold wall in the underlayer fluid begins to grow out and has the tendency to separate into two cells in the left. At $t=\tau_0+1/4\tau_p$, τ_p is the period of oscillation, the cell is divided into two small eddies. One (first eddy) locates at the vicinity of the cold wall, and the other (the second eddy) moves to the position at $x=0.01$ m. Moreover, there is a third eddy found underneath the interface. When $t=\tau_0+1/2\tau_p$, the second eddy travels to the center of the underlayer fluid, and almost occupies the whole domain. At the moment, both the first and third eddies disappear. Thereafter, the primary cell (the second eddy) still migrates continuously toward the right, but it will be drawn back toward the cold wall along the interface after it is fully developed. At $t=\tau_0+3/4\tau_p$, the center of the cell moves to the vicinity of the cold wall, and the peripheral streamlines' structures are separated into a few convective circulations again. It is obvious that there is another convective loop at the corner of the hot wall. Next, the cell near the cold wall will move down, restore back to the initial flow pattern of the τ_0, and start the next oscillatory convection. In the upper layer, the flow consists of a strong eddy attached to the hot wall, and embedded in the return flow is a small region of closed streamlines near the cold side, which is similar to the flow state of oscillatory instability for aspect ratio $\Gamma=4$ as reported by Kuhlmann and Albensoder [11]. From the streamlines' evolution, we know that these cells travel from the cold wall to the hot wall; however, the cell configurations are different from those of the underlayer fluid because the Pr number is different between the upper layer and the underlayer fluids.

That mentioned above is the developing process of the oscillatory wavelike state; it shows that a pair of wave traveling in the x direction formed the two-layer fluid system. This present oscillatory instability is similar with the hydrothermal wave in return flow as reported by S&D [1] due to the thermocapillary effect primarily, but the particular structure of the wave is strongly influenced by the underlying nonparallel basic flow. In order to observe the oscillatory flow much clearly and obtain the exact oscillatory period, we monitored the temperature fluctuation of point P ($x=0.02$ m, $y=0.01$ m, and $z=0.01$ m) with calculating time as shown in Fig. 4. From the figure we can find that the temperature fluctuation is a sinusoid, and the oscillatory period and amplitude become constant after 39.5 s. After that, a periodical temperature wave traveling occurs; it means that the oscillatory instability occurs. The period determined from the temperature oscillation at point P (Fig. 4) is 4.30 s, which is consistent with that found in the temperature wave evolution (Fig. 5).

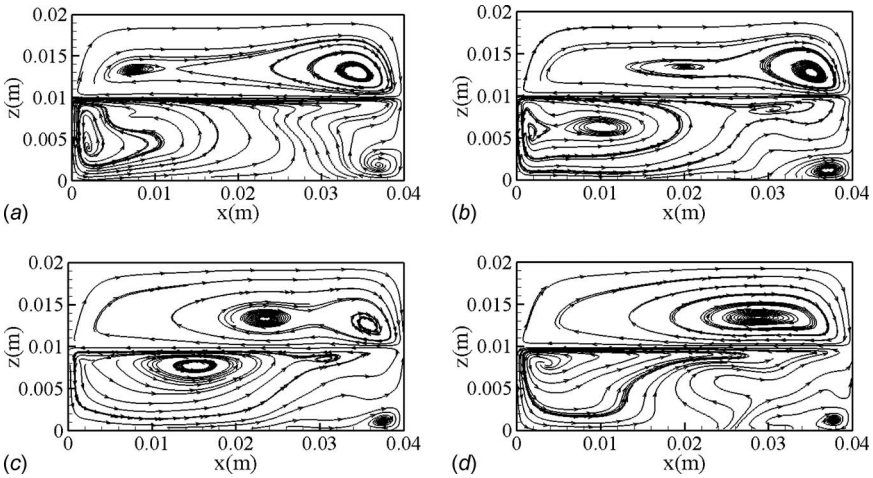

Fig. 3 Streamlines on $y=0.01$ m plane in one oscillation period (τ_p) without MHD: (*a*) $t=\tau_0$, (*b*) $t=\tau_0+1/4\tau_p$, (*c*) $t=\tau_0+1/2\tau_p$, and (*d*) $t=\tau_0+3/4\tau_p$

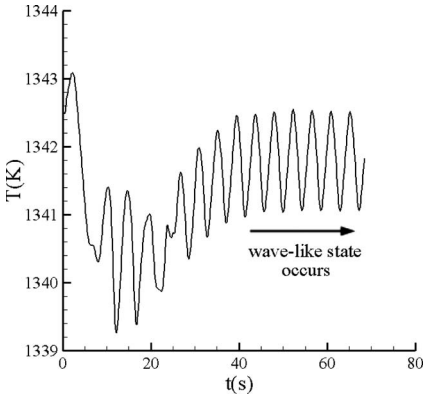

Fig. 4 Temperature fluctuation at the monitoring point *P* with time without MHD

Here, in order to clearly express temporal distributions of temperature disturbances, we introduce a temperature fluctuation function δT [12] for this case, where δT is the deviation of local temperature from time-averaged temperature at that point, defined as $\delta T = T - 1/\tau_p \int_{\tau_0}^{\tau_0+\tau_p} T dt$. Figure 5 indicates a variation of temperature temporal distributions on the $y=0.01$ m plane in one period. The temperature perturbation periodically initiates near the cold wall and propagates from the cold wall to the hot wall, similar to a hydrothermal wave. Its intensity of the temperature perturbation is strengthening gradually during its traveling process. After the temperature wave crest arrives at the hot wall, they are then extruded and die away finally. The range of the temperature fluctuation is -1.0 K to 1.5 K.

4.2 The Impact of Magnetic Fields on Thermocapillary Convection Instability. In order to investigate the effect of a magnetic field on the thermocapillary convection instability, magnetic fields normal to the temperature gradient direction are applied to the system with an intensity of magnetic field varying from 0.01 T to 0.1 T. The corresponding Hartmann number, which represents the ratio of electromagnetic forces to viscous forces, is 11.7 to 117. For the sake of reducing the computation time, in all magnetohydrodynamics (MHD) calculations the magnetic field is applied after the oscillatory convection has formed.

For magnetic field intensity below 0.04 T, the analysis showed that the thermocapillary convection instability in the two-layer fluid system was not suppressed completely and the magnetic field just influenced the period and the amplitude of oscillation. Here, the effects of magnetic field on the wavelike state instability at $B_z=0.04$ T are shown in Fig. 6. When $t=\tau_0$, the convective cell near the cold wall in the underlayer fluid begins to protrude to-

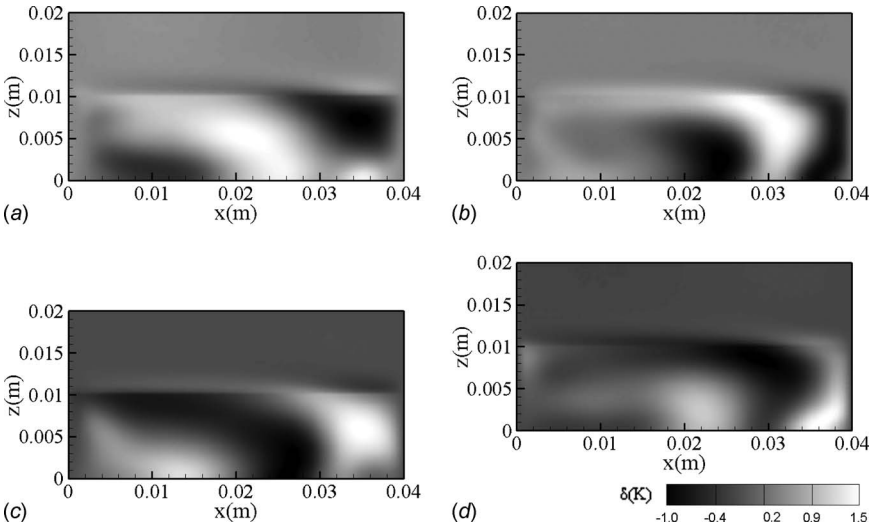

Fig. 5 Temperature temporal perturbation on $y=0.01$ m plane in one period (τ_p) without MHD: (*a*) $t=\tau_0$, (*b*) $t=\tau_0+1/4\tau_p$, (*c*) $t=\tau_0+1/2\tau_p$, and (*d*) $t=\tau_0+3/4\tau_p$

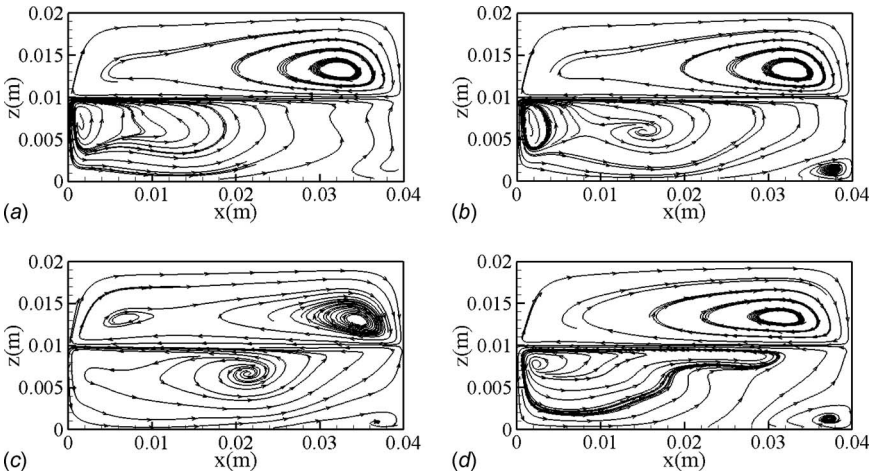

Fig. 6 Streamlines on $y=0.01$ m plane in one oscillation period (τ_p) under $B_z=0.04$ T: (*a*) $t=\tau_0$, (*b*) $t=\tau_0+1/4\tau_p$, (*c*) $t=\tau_0+1/2\tau_p$, and (*d*) $t=\tau_0+3/4\tau_p$

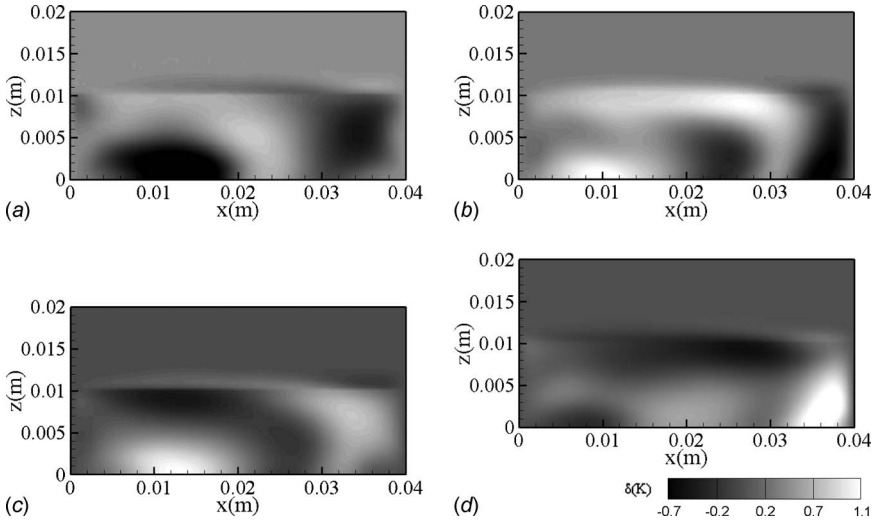

Fig. 7 Temperature perturbation on $y=0.01$ m plane in one period (τ_p) under $B_z=0.04$ T: (*a*) $t=\tau_0$, (*b*) $t=\tau_0+1/4\tau_p$, (*c*) $t=\tau_0+1/2\tau_p$, and (*d*) $t=\tau_0+3/4\tau_p$

ward the right, which makes as starting point of a traveling periodical cell. Comparing with that without a magnetic field, the length of protrusion is shorter, and the distortion of streamlines and the convective eddies are weaker. At $t=\tau_0+1/4\tau_p$, the cell is separated into two small cells. The new cell moves to the position at $x=0.015$ m and the periphery streamlines form an integrated convective circulation, which is faster than that without a magnetic field. At $t=\tau_0+1/2\tau_p$, the cell near the cold wall (old cell) disappears and the new cell becomes the primary convective cell in the underlayer fluid, whose center is closer to the center of the fluid domain compared with that without a magnetic field. The primary cell will contract toward the cold wall along the interface after fully developed and become a smaller cell. When $t=\tau_0+3/4\tau_p$, the cell moves back to the corner between the cold wall and the interface, and the integrated convective circulation is broken. Next, it will redisplay the flow structure of the τ_0 and become the incipience of next traveling after $1/4\tau_p$.

A variation of temperature perturbations on the $y=0.01$ m plane during one period shown in Fig. 7 reveals a similar pattern of temperature wave traveling that found in no magnetic field. The temperature perturbation initiates periodically near the cold wall and propagates toward the hot wall along the temperature gradient direction. However, it should be noticed that the range of temperature oscillation is reduced to −0.7 K to 1.1 K. The temperature perturbation at monitoring point P is shown in Fig. 8 under an applied magnetic field $B_z=0.04$ T. As shown, the period increases slightly to 4.62 s, while the oscillatory amplitude decreases to 1.38 K.

When the magnetic field intensity is increased to 0.05 T, the variation of temperature fluctuations at the monitoring point is not a complete sinusoid as shown in Fig. 9. The oscillatory period and amplitude do not keep constant (see the circle in Fig. 9) and the thermocapillary convection instability becomes more complicated. This means that the oscillation includes several oscillatory frequencies. The temperature fluctuation at the monitoring point under a magnetic field $B_z=0.08$ T is shown in Fig. 10, which displays that the oscillation begins to become irregular and the thermocapillary convection perturbation begins to be annihilated.

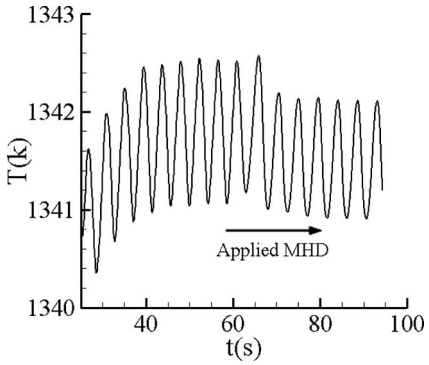

Fig. 8 Temperature fluctuation at monitoring point P under $B_z=0.04$ T

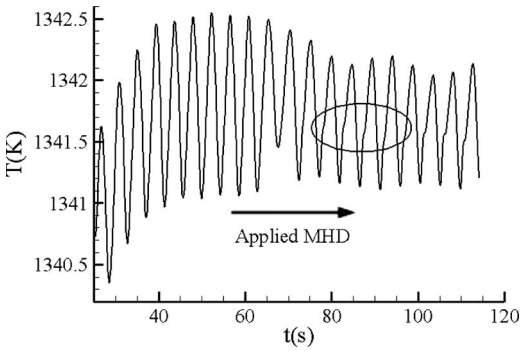

Fig. 9 Temperature fluctuation at point P under $B_z=0.05$ T

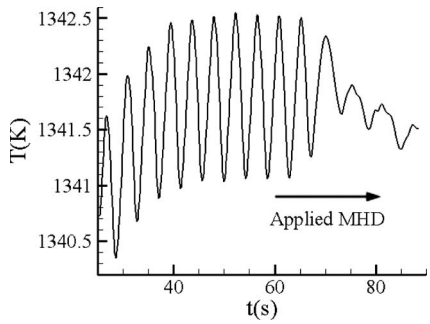

Fig. 10 Temperature fluctuation at point P under $B_z=0.08$ T

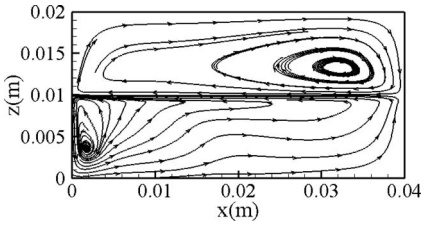

Fig. 11 Steady streamlines' pattern of thermocapillary convection under B_z=0.1 T

When a magnetic field B_z=0.1 T is applied to the two-layer fluid system, the computational results show that the thermocapillary convection does not follow the phenomenon of wavelike state anymore, and the convective configuration is a steady convection cell as shown in Fig. 11. This reveals that the unsteady flow is changed to a steady flow under the normal magnetic field B_z=0.1 T, because the effect of Lorentz forces is stronger than the perturbation effect of thermocapillary forces, then the wave traveling mechanism is suppressed. At the same time, the temperature at the monitoring point P becomes constant gradually, as shown in Fig. 12, which indicates that the oscillatory instability is fully suppressed and the fluid temperature at every point remains constant.

Figure 13 shows that the oscillatory period and oscillatory amplitude vary with Hartmann number at the monitoring point P. From this figure, we understand that the oscillatory period increases slightly with the Hartmann number under lower Hartmann number, but it increases sharply with the Hartmann number approaching 50 or more. Meanwhile, the amplitude of oscillation decreases gradually with the Hartmann number. It indicates that the oscillatory frequency of the wavelike state becomes very slow and the temperature fluctuation is very small under high Hartmann number conditions. Consequently, the unsteady flow is changed to steady flow under a high magnetic field.

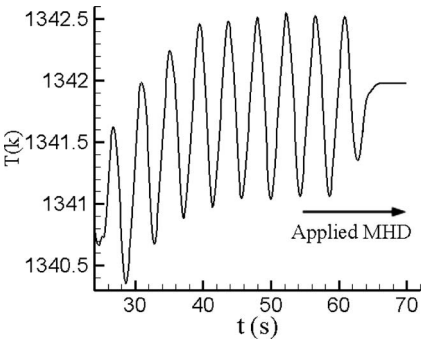

Fig. 12 Temperature fluctuation at monitoring point under B_z =0.1 T

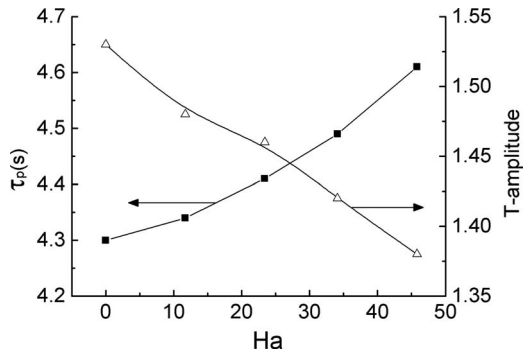

Fig. 13 Oscillatory period and amplitude vary with H_a

5 Conclusions

In this paper, the instability of thermocapillary convection driven by the surface tension gradient and the effects of uniform normal magnetic fields on the convection instability were investigated in the absence of gravity. From the simulation results, the following conclusions are drawn.

(1) In each layer of fluid, the flow cells originate near the cold wall and travel along the temperature gradient direction at $Ma=8.79\times10^4$. It is believed that these moving cells mean that an oscillatory, wavelike state is formed, and this wavelike state is similar with the hydrothermal wave.
(2) When the applied magnetic field B_z is below 0.04 T, the two-layer fluid system still demonstrates a periodic wavelike state, but the oscillatory period increases and the oscillatory amplitude decreases with the increasing of magnetic field intensity. Furthermore, the thermocapillary convection shows no periodic wavelike state instability when $B_z \geq 0.05$ T.
(3) When the intensity of the normal magnetic field is over 0.1 T, the oscillatory instability is fully suppressed, the wavelike state does not occur, and the unsteady thermocapillary convection is transformed into a steady convection flow.

Acknowledgment

The research was supported by the National Natural Science Foundation of China (Grant No. 50576036).

Nomenclature

$\boldsymbol{B}$ = magnetic field intensity (T)
$\boldsymbol{B}_z$ = applied magnetic field intensity (T)
$\boldsymbol{b}$ = induced magnetic field intensity (T)
$\boldsymbol{f}$ = Lorentz force (N m^{-3})
H_a = Hartmann number, $H_a=B_zL\sqrt{\sigma_m/\mu_2}$
$\boldsymbol{J}$ = induced current (A m^{-2})
k = thermal conductivity (W m^{-1} K^{-1})
L = cavity length
M_a = Marangoni number, $M_a=(\partial\sigma_T/\partial T)(T_h-T_c)L/\mu_2\alpha_2$
P = pressure (Pa)
Q = convergence criteria
t = time (s)
T = temperature (K)
u, v, w = velocity components in the (x,y,z) directions

Greek Symbols

α = thermal diffusivity (m^2 s^{-1})
Γ = aspect ratio (the ratio of length to high)
μ = dynamic viscosity (kg s^{-1} m^{-1})
μ_m = magnetic conductivity (henries per meter m^{-1})
ν = kinematic viscosity (m^2 s^{-1})
ρ = density (kg m^{-3})
σ_m = electrical conductivity (Ω^{-1} m^{-1})
σ_T = surface tension (N m^{-1})
τ_p = wave traveling period (s)

Subscripts

i = ith fluid layer (i=1,2)
m = magnetic field
n = normal to the interface

References

[1] Smith, M. K., and Davis, S. H., 1983, "Instabilities of Dynamic Thermocapillary Liquid Layers. Part 1. Convective Instabilities," J. Fluid Mech., **132**, pp. 119–144.
[2] Riley, R. J., and Neitzel, G. P., 1998, "Instability of Thermocapillary–Buoyancy Convection in Shallow Layers. Part 1. Characterization of Steady and Oscillatory Instabilities," J. Fluid Mech., **359**, pp. 143–164.

[3] Xu, J., and Zebib, A., 1998, "Oscillatory Two- and Three-Dimensional Thermocapillary Convection," J. Fluid Mech., **364**, pp. 187–209.
[4] Burguete, J., Mukolobwiez, N., and Daviaud, F., 2001, "Buoyant–Thermocapillary Instabilities in Extended Liquid Layers Subjected to a Horizontal Temperature Gradient," Phys. Fluids, **13**, pp. 2773–2787.
[5] Yang, M., and Ma, N., 2005, "A Computational Study of Natural Convection in a Liquid-Encapsulated Molten Semiconductor With a Horizontal Magnetic Field," Int. J. Heat Fluid Flow, **26**, pp. 810–816.
[6] Morthland, T. E., and Walker, J. S., 1998, "Magnetically Damped Thermocapillary Convections in Fluid Layers in Microgravity," AIAA 98-0653.
[7] Rao, A. R., and Biswal, P. C., 2001, "Benard-Marangoni Convection in Two Thin Immiscible Liquid Layers With a Uniform Magnetic Field," Acta Mech., **151**, pp. 61–73.
[8] Liu, Q. S., Roux, B., and Velarde, M. G., 1998, "Thermocapillary Convection in Two-Layer Systems," Int. J. Heat Mass Transfer, **41**, pp. 1499–1511.
[9] Schwabe, D., and Benz, S., 2002, "Thermocapillary Flow Instabilities in an Annulus Under Microgravity—Results of the Experiment MAGIA," Adv. Space Res., **29**, pp. 629–638.
[10] Leboucher, L., 1999, "Monotone Scheme and Boundary Conditions for Finite Volume Simulation of Magnetohydrodynamic Internal Flows at High Hartmann Number," J. Comput. Phys., **150**, pp. 181–198.
[11] Kuhlmann, H. C., and Albensoder, S., 2008, "Three-Dimensional Flow Instability in a Thermocapillary Driven Cavity," Phys. Rev. E, **77**, p. 036303.
[12] Shi, W. Y., and Nobuyuki, I., 2006, "Hydrothermal Waves in Differentially Heated Shallow Annular Pools of Silicone Oil," J. Cryst. Growth, **290**, pp. 280–291.